Spin-Orbit Effects in the F and K Bands of Colored Alkali Halides*

D. Y. Smith†
Argonne National Laboratory, Argonne, Illinois 60439
and Department of Physics, Michigan State University, East Lansing, Michigan 48823
(Received 17 February 1972)

The effect of the spin-orbit interaction in the bound excited Γ_4^- states of the F center is investigated within the framework of the semicontinuum F-center model. Assuming the K band arises from allowed transitions, expressions for the K-band spin-orbit splitting and the F-K spin-orbit configuration interaction are found using vacancy-centered F-center model wave functions orthogonalized to the core states of neighboring ions. A simple physical picture for the variation of the spin-orbit splitting with state of excitation is developed and the spin-orbit splitting of the highly excited states is shown to vary as the inverse cube of the principal quantum number. A detailed numerical calculation for the RbCl F center is carried out. The predictions include an F-band splitting of -15.3×10^{-3} eV, a K-band splitting of -2.2×10^{-3} eV, and an F-K configuration interaction parameter of -3.8×10^{-3} eV. These results are in good agreement with quantities derived from magneto-optic experiments.

I. INTRODUCTION

The optical absorptions and emissions for electronic transitions of color centers in solids are generally broadened into bands by the electron-phonon interaction. The typical optical spectrum of a color center consequently does not show any of the fine structure that may be present in the center's electronic energy levels. However, in the past few years it has been found that this fine structure may be resolved by external-field techniques.[1-11] These techniques were first applied to the F center in magneto-optical studies that disclosed an unexpectedly large and negative spin-orbit splitting in the F band.[1-10] In addition, these investigations yielded unrelaxed excited-state g factors,[6,9] and the relative contribution of cubic and noncubic lattice vibrations to the broadening of the F band.[11-14]

Spin-orbit structure has also been found in magneto-optic experiments[15-18] on the K-band absorption[19,20] of the F center. This is of particular interest because of the controversy surrounding assignment of this band to specific transitions. In the present paper we shall investigate the theory of spin-orbit effects for this absorption.

Briefly, the K band is a small absorption found in association with the F band in many alkali halides. Typically it lies a few tenths of an eV higher in energy than the F band, but has an oscillator strength roughly one-tenth as great.[19] The K band is best resolved in RbCl, and in those salts in which it is not resolved it probably comprises the long high-energy tail of the F band. There has been much speculation as to the nature of the K absorption, but Chiarotti and Grassano[21] established by modulation of the F-center ground-state population that the K band involves transitions from the F-center ground state. Independent evidence for this is given by the observations of d'Aubigné and Gareyte[15] and of Henry[7] that magneto-optic effects in the K band have the same spin-relaxation time as the F-center ground state.

The situation with respect to the final excited state involved is not as clear. The two most widely discussed models proposed to account for the K band are the following.

(i) The hydrogenic "P-state" or "many-P-state" models that attribute the band to allowed transitions from the F center's "$1s$" (Γ_1^+) ground electronic state to a "$3p$" state or series of "np", $n\geq 3$, states with Γ_4^- symmetry lying below the conduction band, but above the Γ_4^- ($2p$) state responsible for the F band.[20,22]

(ii) The forbidden-transition models in which it is assumed that lattice vibrations mix the Γ_4^- ($2p$) state responsible for the F band with higher-lying even-parity states to which transitions would be otherwise forbidden.[23]

A review of previous studies concerning these and other models has been given by Smith and Spinolo.[20]

In ordinary optical experiments the K band shows no gross structure,[24] but it may be analyzed into two overlapping bands by means of photoconductivity[25,26] or stress measurements.[27] For reference such an analysis is shown in Fig. 1. The lower-energy subband K_1 is the strongest and is centered at the peak of the K band; it has a low photoconductive yield. The much weaker K_2 band lies at higher energies and is reported to have unit quantum yield.[26] In the framework of the allowed-transition model, which we shall adopt here, the K_1 band involves transitions to bound states, primarily the $3p$ (Γ_4^-). The K_2 band then includes transitions to low-lying conduction-band states and the most weakly bound Γ_4^- states which yield conduction electrons by thermal ionization.

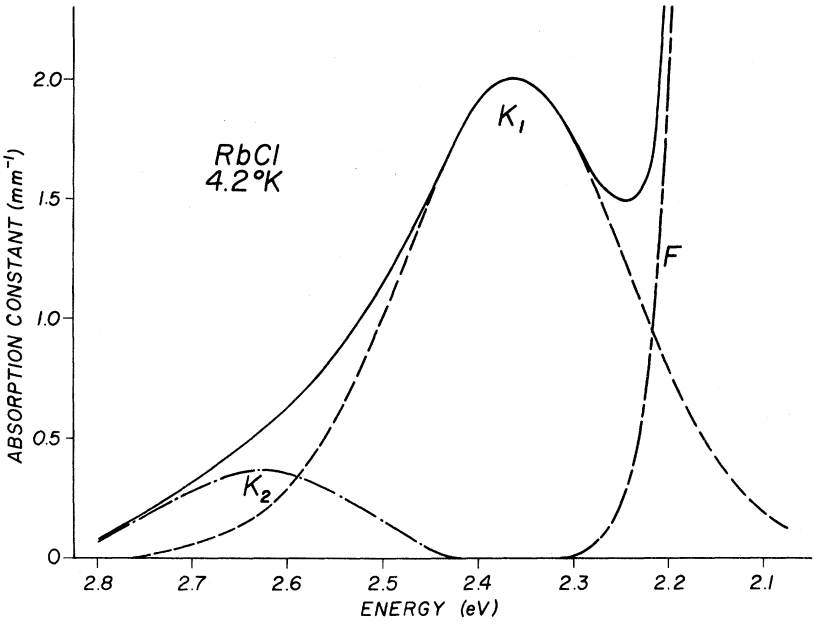

FIG. 1. K band of the F center in RbCl and its analysis into the K_1 and K_2 subbands. After Krätzig and Staude, Ref. 18.

The magneto-optical studies of the K band demonstrate that there is a spin-orbit splitting of the K band[16–18] and a spin-orbit configuration interaction between the final states responsible for the F and K bands.[15,18] The high-resolution measurements of Krätzig and Staude[18] show that these effects are primarily associated with the K_1 subband. However, the interpretation of these results in terms of the proposed K-band models has been the subject of disagreement.[15,16] This stems in part from the lack of estimates of the relevant spin-orbit parameters in the allowed-transition model for comparison with experiment.

The purpose of the present paper is to extend the theory of spin-orbit effects in the F center to the allowed-transition models of the K band. In particular, expressions for the spin-orbit splittings and configuration interaction for the excited P-like states of the semicontinuum model are found and a detailed numerical calculation for the F center in RbCl is carried out. Although primary emphasis is placed on the F center, the theory is general and should apply to a variety of electron-excess defects.

Briefly, our findings are that either of the allowed-transition models for the K band give predictions in good agreement with the observed F- and K-band spin-orbit splittings and the F-K spin-orbit configuration interaction. This agreement, together with the findings that stress experiments are best explained in terms of Γ_4^- final states,[11,27] strengthens the case for believing that the major features of the K band may be explained primarily on the basis of an allowed-transition model.

In Sec. II a brief outline of the theory of the spin-orbit interaction for defects in the orthogonalized vacancy-centered function approach is given. A systematic method of evaluating the relevant lattice sums for the overlap and spin-orbit matrix elements is introduced and a continuum-approximation method of estimating the spin-orbit matrix elements for highly excited states is developed. In Sec. III a numerical example for RbCl is outlined. In Sec. IV a physical picture for the variation of the spin-orbit matrix elements with quantum state is given and in Sec. V the results are discussed in light of the available data. Readers interested in the physics of the problem are urged to read Sec. II up to Eq. (4) and skip immediately to Sec. IV. They will find the intervening details somewhat dull.

II. THEORY

A. Model Wave Functions

In the allowed-transition models the spin-orbit effects in the F and K bands are determined by the spin-orbit matrix elements between the various Γ_4^- levels involved. There have been a variety of calculations of the lowest-lying F-center Γ_4^- state[28,29] and several studies of the next-higher Γ_4^- state.[30] Higher Γ_4^- states have been investigated only in the semicontinuum approximation.[20,31]

In the present work, wave functions found in connection with the study of the K band in RbCl in Ref. 20 will be used. They are the P-like solutions for a spherically symmetric semicontinuum model with a well depth of -5.92 eV, a well radius of $4.1a_0$, and a dielectric constant ϵ of 3.00.

The probability density of some of the low-lying excited states given by these solutions is shown

TABLE I. Distribution of charge in several RbCl F-center states as given by the semicontinuum model for a potential with well depth -5.92 eV, well radius $4.1a_0$, and dielectric constant 3.0.

State	% of charge within vacancy	Radius containing 90% of charge	No. of ions within 90% radius
$1s$	91	$6a_0$	0
$2p$	24	$18a_0$	92
$3p$	5	$46a_0$	1742
$4p$	2	$84a_0$	10500

in Fig. 2. Since the states of interest are those in absorption, effects of lattice relaxation following absorption are not included. Table I summarizes the properties of these states. It will be seen that the model predicts a ground state largely contained within the vacancy in qualitative agreement with magnetic-resonance measurements.[32] The first excited P state is partly inside the vacancy and partly outside as found in other F-center model calculations.[28] The np states for $n \geq 3$ have very little charge within the vacancy and approach hydrogenic functions for large n as expected for shallow-donor states.[20,33]

B. Spin-Orbit Effects in Compact States

The spin-orbit effects in the F center have been shown to arise from the strong electric fields near the nuclei of the neighboring ions.[34] A quantitative description of these effects has been developed[34,35] starting from a vacancy-centered model wave function (of the sort described above) and requiring that the Pauli principle be satisfied by orthogonalizing this function to the occupied states of the crystal ions. The major steps in this procedure are outlined below.

If the overlap of the ion-core wave functions φ_α with one another is neglected, the orthogonalized wave function of the F-center electron ϕ_i is given by Schmidt orthogonalization of the F-center-model P function u_i to the states φ_α. Thus,

$$\phi_i = (1 - \textstyle\sum_\alpha S^2_{\alpha,i})^{-1/2}(u_i - \sum_\beta S_{\beta,i}\varphi_\beta), \tag{1}$$

where $S_{\alpha,i}$ is the overlap integral $\langle \varphi_\alpha | u_i \rangle$ and the sums over α and β range over all occupied core states.

The spin-orbit interaction is given in general by[36]

$$h_{so} = -e(2m^2c^2)^{-1}\vec{S}\cdot(\vec{E}\times\vec{p}), \tag{2}$$

where e is the electronic charge (a negative number), m the mass of the electron, c the velocity of light, $\vec{S}$ the spin operator, $\vec{p}$ the linear momentum operator, and $\vec{E}$ the electric field through which the electron moves. Since the electric fields are large only near the nuclei of the ions, the interaction is to a good approximation

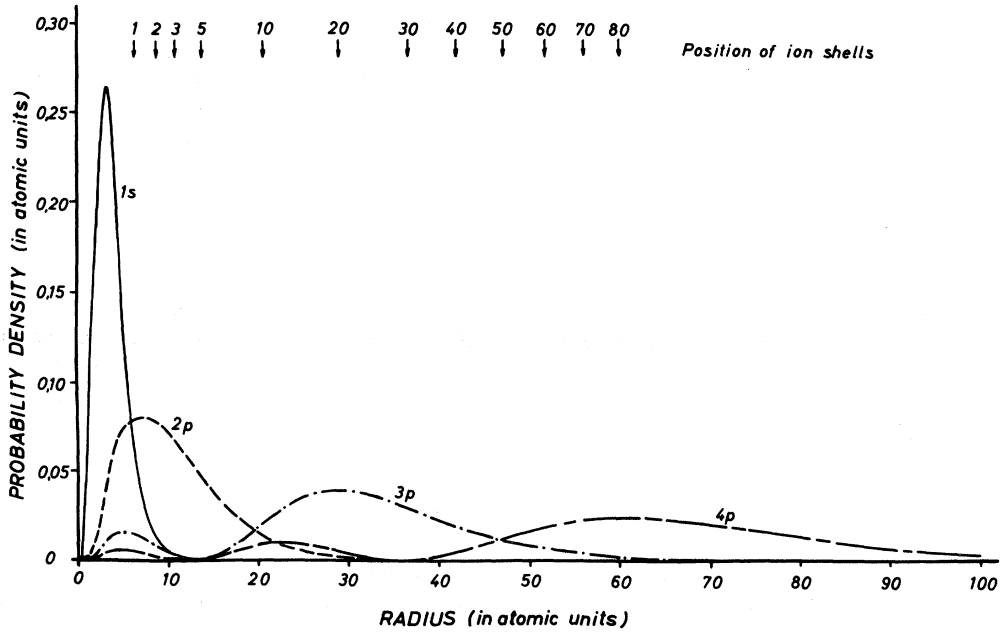

FIG. 2. Radial probability distribution for several of the lowest states of the F center in the semicontinuum model. These states were calculated for a Simpson potential with a well radius of $4.1a_0$, a well depth of -5.92 eV, and a dielectric constant of 3.0 (see Ref. 20 for details). The arrows give the position of the indicated shells of ions. Note that the ground $1s$ state is almost completely within the vacancy, whereas the $4p$ state has its maximum beyond the 80th shell of neighbors.

$$h_{so} = (2m^2c^2)^{-1} \sum_I (|\vec{r} - \vec{R}_I|)^{-1} \frac{\partial V_I}{\partial(|\vec{r} - \vec{R}_I|)} \vec{L}_I \cdot \vec{S}$$
$$= \sum_I \xi(|\vec{r} - \vec{R}_I|) \vec{L}_I \cdot \vec{S}, \quad (3)$$

where the index I labels the ion at point $\vec{R}_I$ and V_I is the potential of an electron in the field of the Ith ion. Here the orbital angular momentum is measured with respect to the Ith nucleus so that $\vec{L}_I = (\vec{r} - \vec{R}_I) \times \vec{p}$.

The matrix elements of the spin-orbit interaction for the orthogonalized F-center functions are then given by[37]

$$\langle \phi_i | h_{so} | \phi_j \rangle = N_i N_j [\langle u_i | h_{so} | u_j \rangle - \sum_\alpha S_{i,\alpha} \langle \varphi_\alpha | h_{so} | u_j \rangle - \sum_\beta S_{\beta,j} \langle u_j | h_{so} | \varphi_\beta \rangle + \sum_{\alpha,\beta} S_{i,\alpha} S_{\beta,j} \langle \varphi_\alpha | h_{so} | \varphi_\beta \rangle], \quad (4)$$

where N_i is the normalization factor $(1 - \sum_\alpha S^2_{\alpha,i})^{-1/2}$. Subsequently, the term $\langle u_i | h_{so} | u_j \rangle$ involving just vacancy-centered functions will be referred to as the "vacancy-vacancy" term. Terms involving $\langle \varphi_\alpha | h_{so} | u_j \rangle$ will be referred to as "vacancy-ion" cross terms, and terms of the third type, $\langle \varphi_\alpha | h_{so} | \varphi_\beta \rangle$, will be called "ion-ion" terms.

The evaluation of the sums over crystal ions in Eq. (4) and in the normalization can be greatly simplified if the ions in each of the various shells of neighbors are treated as separate groups. The simplification arises because the contribution of a given ion may be written as products of the ion's direction cosines times overlap and spin-orbit matrix elements which depend only on the radius of the ion shell in question.[38] For lattices of high symmetry, the sum over ions in a given shell corresponds to a permutation of the direction cosines, and the Pythagorean theorem may be used to reduce the sum to a numerical factor times the matrix elements.

In the normalization sums of terms involving products of overlap integrals arise. These are evaluated in Appendix A for an NaCl-type lattice. In the case of a normalized P-like vacancy-centered function the sums of the products of the overlap integrals for the n ions in a *single* shell of neighbors are found to be

S-like core states,

$$\sum'_\alpha S_{i,\alpha} S_{\alpha,j} = \tfrac{1}{3} n \sum''_\alpha S(p_i, s_\alpha\sigma) S(p_j, s_\alpha\sigma); \quad (5)$$

P-like core states,

$$\sum'_\alpha S_{i,\alpha} S_{\alpha,j} = \tfrac{1}{3} n \sum''_\alpha [S(p_i, p_\alpha\sigma) S(p_j, p_\alpha\sigma) + 2S(p_i, p_\alpha\pi) S(p_j, p_\alpha\pi)]; \quad (6)$$

D-like core states,

$$\sum'_\alpha S_{i,\alpha} S_{\alpha,j} = \tfrac{1}{3} n \sum''_\alpha [S(p_i, d_\alpha\sigma) S(p_j, d_\alpha\sigma) + 2S(p_i, d_\alpha\pi) S(p_j, d_\alpha\pi)]. \quad (7)$$

Here the notation $\sum'_\alpha$ on the left-hand side of these equations indicates a sum over the core states of *all* the ions in a single shell containing n ions. The sum $\sum''_\alpha$ on the right-hand side indicates a sum over the various σ and π overlap integrals for a *single* ion in the shell. The overlap integral $S(p_i, s_\alpha\sigma)$ is the σ overlap of the ith P-like F-center model wave function and the S-like core state φ_α of a single ion in the shell. Similarly, $S(p_i, p_\alpha\sigma)$ and $S(p_i, p_\alpha\pi)$ are the σ and π overlap integrals with P-like core states, and $S(p_i, d_\alpha\sigma)$ and $S(p_i, d_\alpha\pi)$ are the σ and π overlap integrals with D-like core states. For ease in computation, these are defined in terms of real spherical harmonics as outlined in Appendix A.

The spin-orbit splitting of the Γ_4^- state is conveniently evaluated by calculating the spin-orbit matrix elements for the $\Gamma_8^-(P_{3/2})$-symmetry vacancy-centered state u_i having the form $(3/8\pi)^{1/2} \mathcal{R}_i(r) [(x+iy)/r] \uparrow$, where $\uparrow$ is the spin-up spinner. In a simple atomic picture this is the P state with total angular momentum J equal to $\frac{3}{2}$ and projected angular momentum m_J equal to $\frac{3}{2}$. The evaluation proceeds in a manner similar to that for the overlap integrals and is outlined in Appendix B. The result for the vacancy-vacancy term in Eq. (4) is

$$\langle u_i | h_{so} | u_j \rangle = n(\lambda_{ss} + R\lambda_{sp\,\sigma}/\sqrt{3}), \quad (8)$$

where R is the radius of the shell of neighbors in question, and λ_{ss} and $\lambda_{sp\,\sigma}$ are spin-orbit integrals involving the charge distribution $\mathcal{R}_i(r)\mathcal{R}_j(r)$ centered on the vacancy and the spin-orbit interaction of an ion. Their explicit forms are given in Appendix B by Eqs. (B9) and (B11).

The vacancy-ion cross terms in Eq. (4) are

P-like core functions,[39]

$$\sum'_\alpha S_{\alpha,i} \langle u_j | h_{so} | \varphi_\alpha \rangle = \tfrac{1}{3} n \sum''_\alpha [S(p_i, p_\alpha\pi) \lambda(p_j, p_\alpha\pi) + S(p_i, p_\alpha\pi) \lambda(p_j, p_\alpha\sigma) + S(p_i, p_\alpha\sigma) \lambda(p_j, p_\alpha\pi)]; \quad (9)$$

D-like core functions,

$$\sum'_\alpha S_{\alpha,i} \langle u_j | h_{so} | \varphi_\alpha \rangle = \tfrac{1}{3} n \sum''_\alpha [S(p_i, d_\alpha\pi) \lambda(p_j, d_\alpha\pi) + \sqrt{3}\, S(p_i, d_\alpha\pi) \lambda(p_j, d_\alpha\sigma) + \sqrt{3}\, S(p_i, d_\alpha\sigma) \lambda(p_j, d_\alpha\pi)], \quad (10)$$

where the integrals $\lambda(p_j, p_\alpha\pi)$, etc., are spin-orbit overlap integrals that are similar to the corresponding $S(p_j, p_\alpha\pi)$, etc., but with an additional factor of the ionic spin-orbit interaction in the integrand. They are given in Appendix B by Eqs. (B15) and (B16).

The ion-ion terms of Eq. (4) are similar in form to Eqs. (9) and (10), but are quadratic in the overlap integrals. They are given by

P-like core states,[39]

$$\sum_{\alpha\beta}{}' S_{i,\alpha} S_{\beta,j} \langle \varphi_\alpha | h_{so} | \varphi_\beta \rangle = \tfrac{1}{3} n \sum_{\alpha,\beta}{}'' \lambda_{\alpha\beta} [S(p_i, p_\alpha \pi) \times S(p_j, p_\beta \pi) + S(p_i, p_\alpha \pi) S(p_j, p_\beta \sigma) + S(p_i, p_\alpha \sigma) S(p_j, p_\beta \pi)] ; \quad (11)$$

D-like core states,

$$\sum_{\alpha\beta}{}' S_{i,\alpha} S_{\beta,j} \langle \varphi_\alpha | h_{so} | \varphi_\beta \rangle = \tfrac{1}{3} n \sum_{\alpha,\beta}{}'' \lambda_{\alpha\beta} [S(p_i, d_\alpha \pi) \times S(p_j, d_\beta \pi) + \sqrt{3} S(p_i, d_\alpha \pi) S(p_j, d_\beta \sigma) + \sqrt{3} S(p_i, d_\alpha \sigma) S(p_j, d_\beta \pi)] , \quad (12)$$

where the $\lambda_{\alpha\beta}$ are ionic spin-orbit matrix elements given explicitly by Eq. (B19).

The existence of these sum rules for ions within a given shell simplifies the problem considerably because the ions in a shell may be treated as a group without knowing their specific arrangement.

C. Continuum Approximation for Diffuse States

The number of ions overlapped by an excited-state wave function increases rapidly with quantum number, making it impractical to consider an orthogonalized vacancy-centered function (OVCF) calculation for all but the lowest levels. However, the diffuse nature of the higher excited states may be exploited to develop an alternative approach to estimating spin-orbit energies for these levels.

Here the aim is to find expressions for the overlap and spin-orbit matrix elements for a given state in terms of its quantum numbers and adjustable parameters which may be fixed by a full OVCF calculation for a low-lying excited state. The basic motivation is that for diffuse states overlap and spin-orbit matrix elements involving neighboring ions may be related to the amplitude and slope of the model wave function at the ion in question. Further, the sum over crystal ions may be replaced approximately by an integration. The expressions for the spin-orbit matrix elements given in Sec. IIB are then found to yield simple expressions similar to those for atomic hydrogen.

To proceed we observe that in the case of a diffuse-model wave function which varies sufficiently slowly over the dimensions of an ion, the overlap integrals may be calculated approximately by expanding the model wave function in a Taylor series about the nucleus of the ion in question. For σ overlap with P-like core functions the major contribution to the overlap integrals is determined by the term in the first derivative. Writing the wave function $u_i(\vec{r})$ as $\mathcal{R}_i(r) Y_1^m(\theta, \Phi)$, where $\mathcal{R}_i(r)$ is the radical part and $Y_1^m(\theta, \Phi)$ the appropriate spherical harmonic, we have for ions on a shell of radius r'

$$S(p_i, p_\alpha \sigma) \approx (3/4\pi)^{1/2} C_{\alpha\sigma} \mathcal{R}_i'(r') . \quad (13)$$

This gives the σ overlap with core state φ_α as a function of shell radius in terms of the derivative of the radial part of the model wave function and a constant $C_{\alpha\sigma}$. The latter will actually be a constant for a given ionic core state only if the variation of the wave function over the ion cores is given by the first few terms in the Taylor expansion. For π overlap integrals the constant term in the expansion is the major contributor, yielding

$$S(p_i, p_\alpha \pi) \approx (3/4\pi)^{1/2} C_{\alpha\pi} \mathcal{R}_i(r')/r' . \quad (14)$$

The C's in Eqs. (13) and (14) are conveniently defined for an ion on the z axis, i.e., at the point $\vec{r} = r'\hat{k}$, by the expressions

$$C_{\alpha\sigma} = \int \varphi^*_{\alpha,(z-r')}(\vec{r} - r'\hat{k})(z - r') \, d^3r \quad (15)$$

and

$$C_{\alpha\pi} = \int \varphi^*_{\alpha,x}(\vec{r} - r'\hat{k}) \, x \, d^3r . \quad (16)$$

Here the core function $\varphi_\alpha(\vec{r})$ transforming like x is denoted by $\varphi_{\alpha,x}(\vec{r})$, etc.

As a test of this approximation the values of $C_{\alpha\sigma}$ and $C_{\alpha\pi}$ were calculated from overlap integrals for the NaCl F-center $2p$ function with Na^+ $2p$ core functions at distances of $5.3a_0$ and $9.2a_0$.[34] It was found that even for the relatively compact $2p$ F-center state, the major variation in overlap arises from the spatial variation in $\mathcal{R}'(r)$ and $\mathcal{R}(r)/r$. For example, although S_σ changed by a factor of 4 between the two sites, $C_{Na^+ 2p\sigma}$ was constant to within 1%. Similarly, the factor of 10 variation in S_π was accounted for to within 20% by Eq. (14). For the far more diffuse higher excited states the approximations of Eqs. (13) and (14) should be considerably better.

By a change of variables it may be shown that $C_{\alpha\sigma}$ and $C_{\alpha\pi}$ are rigorously equal to one another. This is only approximately true for the "empirical" values found from Eqs. (13) and (14) by using the actual overlap integrals. This difference arises because of the truncation of the Taylor expansion. We shall therefore consider the C's as empirical coefficients defined by Eqs. (13) and (14).

A further simplification arises because the overwhelming contribution to the spin-orbit interaction arises from the ion-ion term for overlap with P-like core states, Eq. (11). As will become apparent in Sec. III, the ion-ion term for the P core states accounts for all but a few tenths of a percent of the spin-orbit interaction in both the $2p$ and $3p$ states of the RbCl F center. Similar results hold for the $2p$-$3p$ configuration interaction in RbCl and the NaCl F-band splitting.[34]

Using Eqs. (13) and (14) and neglecting all but the ion-ion terms, the matrix elements between Γ_8^- ($P_{3/2}$) states become

$$\langle \phi_i | h_{so} | \phi_j \rangle_{3/2,3/2} = \frac{N_i N_j}{4\pi}$$

$$\times \sum_{\substack{i \\ \text{shells}}} n_i \Big[\Big(\sum_{\alpha,\beta} C_{\alpha\pi} C_{\beta\pi} \lambda_{\alpha\beta} \Big) \mathcal{R}_i(r_i') \mathcal{R}_j(r_i') / r_i'^2$$

$$+ \Big(\sum_{\alpha,\beta} C_{\alpha\pi} C_{\beta\sigma} \lambda_{\alpha\beta} \Big) \mathcal{R}_i(r_i') \mathcal{R}_j'(r_i') / r_i'$$

$$+ \Big(\sum_{\alpha,\beta} C_{\alpha\sigma} C_{\beta\pi} \lambda_{\alpha\beta} \Big) \mathcal{R}_i'(r_i') \mathcal{R}_j(r_i') / r_i' \Big] . \quad (17)$$

Here a subscript $\frac{3}{2}$, $\frac{3}{2}$ has been added to the matrix elements to indicate that the $P_{3/2}$ states are involved. In the limit of diffuse wave functions the sum over shells may be replaced by an integral and the terms involving $\mathcal{R}'(r_i')$ may be integrated by parts. This yields

$$\langle \phi_i | h_{so} | \phi_j \rangle_{3/2,3/2}$$

$$= \rho N_i N_j \sum_{\alpha,\beta} (C_{\alpha\pi} C_{\beta\pi} - C_{\alpha\pi} C_{\beta\sigma}) \lambda_{\alpha\beta} \int_0^\infty \mathcal{R}_i(r') \mathcal{R}_j(r') \, dr', \quad (18)$$

where ρ is the density of ions in the crystal.

For $i=j$ this may be evaluated on the assumption that the F-center wave functions are approximately those of an electron bound to a unit point charge in a dielectric medium with dielectric constant ϵ. The result is[40]

$$\langle \phi_i | h_{so} | \phi_i \rangle_{3/2,3/2}$$

$$= \left(\frac{2\rho N_i^2}{3a_0^2} \sum_{\alpha,\beta} (C_{\alpha\pi} C_{\beta\pi} - C_{\alpha\pi} C_{\beta\sigma}) \lambda_{\alpha\beta} \right) \epsilon^{-2} n_i^{-3}, \quad (19)$$

where n_i is the principal quantum number of the F-center P state considered. This result is probably best interpreted as indicating that

$$\langle \phi_i | h_{so} | \phi_i \rangle_{3/2,3/2} \approx k_\mu / \epsilon^2 n_i^3, \quad (20)$$

where k_μ is an effective spin-orbit parameter to be evaluated from an OVCF calculation for a state of sufficiently high principal quantum number μ so that the continuum assumptions are reasonably well satisfied. The detailed calculations of Sec. III yield spin-orbit splittings of -15.3 and -3.24 meV for the RbCl F-center $2p$ and $3p$ states, respectively. Evaluation of k_μ from these yields

$$k_{2p}/\epsilon^2 = -40.9 \times 10^{-3} \text{ eV}$$

and

$$k_{3p}/\epsilon^2 = -29.1 \times 10^{-3} \text{ eV}.$$

Since the $2p$ state is not sufficiently diffuse for continuum theory to apply, it is not surprising that these two values differ. However, it is noteworthy that the major part—73% in this example—of the change in spin-orbit interaction between the $2p$ and $3p$ states is accounted for by the n^{-3} dependence even for these relatively compact states. Since the $3p$ state is the most diffuse state which could be handled conveniently, we shall use k_{3p} for estimating the spin-orbit interaction from Eq. (20) for $n \geq 4$.

The n^{-3} dependence is striking since it is the same as that for a simple alkali atom.[16,41] Equation (20) also indicates how sensitive the spin-orbit splittings of the higher states are to the choice of dielectric constant used in the semicontinuum model.

In the case of the off-diagonal $2p$-np matrix elements the continuum approximation is probably not reliable because the $2p$ state is relatively compact. However, the similarity in the values of k_{2p} and k_{3p} suggests that the state may be sufficiently hydrogenic to warrant the use of this approximation to estimate the higher off-diagonal terms from the results of a detailed OVCF calculation of $\langle \phi_{2p} | h_{so} | \phi_{3p} \rangle$.

The result for off-diagonal terms corresponding to Eq. (20) is

$$\langle \phi_{2p} | h_{so} | \phi_{np} \rangle_{3/2,3/2} \approx k_{2p,np} \tfrac{3}{2} a_0^2 \int_0^\infty \mathcal{R}_{2p}(r') \mathcal{R}_{np}(r') \, dr', \quad (21a)$$

where

$$k_{2p,np} = \frac{2\rho N_{2p} N_{np}}{3a_0^2} \sum_{\alpha,\beta} (C_{\alpha\pi} C_{\beta\pi} - C_{\alpha\pi} C_{\beta\sigma}) \lambda_{\alpha\beta} . \quad (21b)$$

Assuming hydrogenic wave functions, the integral in Eq. (21a) may be evaluated from the explicit expression for the Laguerre polynomials.[40] This yields

$$\tfrac{3}{2} a_0^2 \int_0^\infty \mathcal{R}_{2p}(r') \mathcal{R}_{np}(r') \, dr' = \epsilon^{-2} \frac{24}{\sqrt{6}} \left(\frac{n(n+1)}{n-1} \right)^{1/2}$$

$$\times \sum_{\lambda=0}^{n-2} \frac{(-4)^\lambda (\lambda+1)(\lambda+2)}{(n-2-\lambda)\,!\,(3+\lambda)\,!\,(2+n)^{\lambda+3}} . \quad (22)$$

The quantity $k_{\mu\nu}$ corresponds to k_μ of Eq. (20) and should be considered as an empirical constant to be evaluated from the detailed calculation of $\langle \phi_\mu | h_{so} | \phi_\nu \rangle$. Using Eq. (22) and the $2p$-$3p$ spin-orbit matrix element for the RbCl F center yields

$$k_{2p,3p}/\epsilon^2 = -93.6 \times 10^{-3} \text{ eV}.$$

For purely hydrogenic functions, $k_{2p,np}$ is independent of n except for small changes in the normalization N_{np},[42] and should be approximately equal to k_μ of Eq. (20). However, the calculated value is a factor of 2–3 times larger than the values of k_{2p}/ϵ^2 and k_{3p}/ϵ^2, indicating that, while the continuum approximation gives order-of-magnitude estimates of the matrix elements, it may be in considerable error when a compact state is involved as in the $2p$-np matrix elements. However, as will be seen in Sec. III, the F-K spin-orbit configuration interaction is dominated by the $2p$-$3p$ term, so that approximating $k_{2p,np}$ by $k_{2p,3p}$ suffices for estimating the small correction terms arising from configuration interaction with higher excited states.

D. Orthogonalization of Higher Excited States

Thus far we have not considered the orthogonality of the various functions ϕ_i obtained from Eq. (1). In general these functions are not orthogonal if they have the same symmetry. To rectify this one might envisage making an OVCF calculation for the various Γ_4^- states in the following manner: First calculate ϕ_{2p} by orthogonalizing u_{2p} to the lattice states by using Eq. (1). Then calculate a trial function for the next-higher state $\phi_{3p}^{(1)}$ by applying Eq. (1) to u_{3p}. In general, ϕ_{2p} and $\phi_{3p}^{(1)}$ have nonzero overlap, but they may be orthogonalized by a further application of the Schmidt procedure to $\phi_{3p}^{(1)}$ to find the orthonormalized state ϕ_{3p}. This leads to

$$\phi_{3p} = (1 - \mathfrak{S}_{2p,3p}^2)^{-1/2} (\phi_{3p}^{(1)} - \mathfrak{S}_{2p,3p}\phi_{2p}), \tag{23}$$

where

$$\phi_{3p}^{(1)} = (1 - \textstyle\sum_\alpha S_{\alpha,3p}^2)^{-1/2} (u_{3p} - \sum_\beta S_{\beta,3p}\varphi_\beta) \tag{24}$$

and

$$\mathfrak{S}_{2p,3p} = \langle \phi_{2p} | \phi_{3p}^{(1)} \rangle = -N_{2p}N_{3p}\textstyle\sum_\alpha S_{2p,\alpha}S_{\alpha,3p}. \tag{25}$$

The diagonal $3p$ spin-orbit matrix element is then

$$\begin{aligned}\langle \phi_{3p} | h_{so} | \phi_{3p} \rangle = (1 - \mathfrak{S}_{2p,3p}^2)^{-1} (&\langle \phi_{3p}^{(1)} | h_{so} | \phi_{3p}^{(1)} \rangle \\ &- \mathfrak{S}_{3p,2p}\langle \phi_{2p} | h_{so} | \phi_{3p}^{(1)} \rangle \\ &- \mathfrak{S}_{2p,3p}\langle \phi_{3p}^{(1)} | h_{so} | \phi_{2p} \rangle \\ &+ \mathfrak{S}_{2p,3p}^2\langle \phi_{2p} | h_{so} | \phi_{2p} \rangle).\end{aligned} \tag{26}$$

Similarly, the $2p - 3p$ configuration matrix element is

$$\begin{aligned}\langle \phi_{2p} | h_{so} | \phi_{3p} \rangle = (1 - \mathfrak{S}_{2p,3p}^2)^{-1/2} (&\langle \phi_{2p} | h_{so} | \phi_{3p}^{(1)} \rangle \\ &- \mathfrak{S}_{2p,3p}\langle \phi_{2p} | h_{so} | \phi_{2p} \rangle).\end{aligned} \tag{27}$$

A similar sequence of orthogonalizations first to the lattice ions and then to lower-lying states could be carried out for the higher P states.

Evaluation of the overlap matrix element $\mathfrak{S}_{2p,3p}$ for the semicontinuum-model functions of the RbCl F center gives a value of approximately -1×10^{-2}. This is essentially the limit of computational accuracy and will be seen to give only small corrections to the matrix elements. The reason this overlap is so small is that it is given by the sum of the products of the core overlaps with the u's involved. These overlap matrix elements reflect the oscillations of the radial part of the u's as an alternation in the signs of the terms in the sum on the right-hand side of Eq. (25). It is the oscillation in the u's that orthogonalize the various u's to one another, so it is not surprising that the alternation of the signs of the products in Eq. (25) leads to almost complete cancellation in the sum. This should hold equally well for higher excited states.

In the numerical example discussed in Sec. III the $3p$ matrix elements are corrected according to Eqs. (26) and (27). The correction is ignored for the higher states. This should be a particularly good assumption since the major contribution to the oscillator strength of the K band appears to come from the $3p$ state.[20] Thus, the slight lack of orthogonality of the higher states should have negligible influence on the total spin-orbit effects.

A possible objection to the present treatment for diffuse wave functions and for the tails of the more compact states is that the wave functions found by solving the Schrödinger equation for the semicontinuum model are really envelope functions in the continuum region of the model potential.[33] In this region the wave functions should be multiplied by a Bloch function of the conduction band. Since the functions of interest are diffuse, only Bloch functions of small wave vector k will be important for the problem and we are at liberty to construct these by the OPW method.[43] Multiplying the envelope function with an OPW for small k then yields a wave function that is equivalent, within the effective-mass approximation, to the orthogonalized vacancy-centered function we have used.

III. NUMERICAL EXAMPLE FOR RbCl

The overlap and spin-orbit matrix elements for the RbCl F center were numerically evaluated using the $2p$ and $3p$ F-center wave functions found by Smith and Spinolo.[20] The crystal-ion core states were approximated by the free-ion Hartree-Fock functions reported by Watson and Freeman[44] for Rb^+ and by Hartree and Hartree[45] for Cl^-. In evaluating the various lattice sums sufficient shells were included so that the contributions from the ions in the outermost shell were of the order of 10^{-2} or less of those from the first two shells of neighbors. For the $2p$ state 20 shells of neighbors (460 ions) were included in the calculation and for the $3p$ state the calculation was carried to the 85th shell (4168 ions). In the case of the $2p - 3p$ off-diagonal matrix elements 40 shells (1356 ions) were included. As will be seen from Fig. 2 and Table I, these shells include at least 98% of the particular electronic charge density under consideration.

The results of the calculation are summarized in Tables II and III, which give the spin-orbit splittings and spin-orbit configuration interaction parameters for the various states. The spin-orbit splitting Δ is defined in analogy with the atomic case as the separation of the Γ_6^- ($P_{1/2}$) and the Γ_8^- ($P_{3/2}$) multiplets. The negative splitting is characteristic of F centers and indicates that the Γ_6^- ($P_{1/2}$) state lies above the Γ_8^- ($P_{3/2}$) in energy.

In terms of the matrix elements for the state with

TABLE II. Calculated spin-orbit splittings Δ_{np} of excited F-center states in RbCl. The ratio of the oscillator strength of the individual transitions to the total K-band oscillator strength is denoted by f_n/f_K and is the weighting factor used to determine the apparent average spin-orbit splitting of the K band. Values of f_n are taken from Ref. 20 and f_K is taken as $\sum_{n=3}^{\infty} f_n$.

Electronic state	Δ_{np} (meV)	f_n/f_K
$2p$	−15.3	...
$3p$	−3.2	0.5691
$4p$	−1.4	0.1886
$5p$	−0.70	0.0863
$6p$	−0.41	0.0465
$7p$	−0.26	0.0278
$8p$	−0.17	0.0186
$9p$	−0.12	0.0126
$10p$	−0.09	0.0093
$11p$	−0.07	0.0066
$12p-\infty p$	...	0.0345

$J=\frac{3}{2}$, $m_J=\frac{3}{2}$, $\phi_{np}^{3/2,3/2}$ used in Sec. II, we have

$$\Delta_{np}=3\langle \phi_{np}^{3/2,3/2}|\, h_{so}\,|\phi_{np}^{3/2,3/2}\rangle \ . \tag{28}$$

The spin-orbit configuration interaction parameter is also conveniently defined in terms of the off-diagonal matrix elements between the $J=\frac{3}{2}$, $m_J=\frac{3}{2}$ states for different configurations as[46]

$$\xi_{np,mp}=2\langle \phi_{np}^{3/2,3/2}|\, h_{so}\,|\phi_{mp}^{3/2,3/2}\rangle \tag{29a}$$

or, by substituting for h_{so} from Eq. (3), as

$$\xi_{np,mp}=\sum_I \langle \phi_{np}^{3/2,3/2}|\, \xi(r-R_I)\, L_z\,|\phi_{mp}^{3/2,3/2}\rangle \ . \tag{29b}$$

The inclusion of the factor of 2 in the first form, Eq. (29a), serves to eliminate the spin expectation value so that ξ_{np-mp} is an expectation value of space operators without any constant factors (this choice is made to simplify subsequent formulas; see Sec. V).

In Table II the calculated values of the $2p$ and $3p$ spin-orbit splittings are listed together with approximate splittings for the higher excited states as estimated from Eq. (20) using k_{3p}. The third column gives the relative contribution of the various P states to the area of a composite K band consisting of transitions to all bound np, $n\geq 3$, states as calculated from the oscillator strengths given in Ref. 20. The configuration interaction matrix elements are listed in Table III. These include the calculated $2p$-$3p$ interaction parameter and the $2p$-np parameters derived form $k_{2p,3p}$ by use of Eq. (21). A detailed comparison of these results with experiment is given in Sec. V.

The normalization and spin-orbit matrix elements used in finding Δ_{np} and $\xi_{2p,3p}$ are listed for reference in Table IV. In the case of the $3p$-$3p$ and $2p$-$3p$ matrix elements two totals are given. They differ by the correction for $2p$-$3p$ overlap given by Eqs. (26) and (27), which amounts to a 2–4% effect.

A number of simplifying assumptions that limit the accuracy of the predictions are involved in the present treatment. One of the major approximations is the use of semicontinuum-model wave functions. An estimate of the uncertainty in the predicted matrix elements arising from the uncertainty in the model dielectric constant may be made from Eq. (20). The wave functions were derived for $\epsilon=3$. However, the optical dielectric constant of RbCl is 2.19 and the static dielectric constant[47] is 5.0, so that a range in ϵ of perhaps 2.19 to about 4 is not unreasonable if other model potentials are varied accordingly.[48] In the continuum approximation of Eq. (20), this range in ϵ gives spin-orbit matrix elements greater or less by a factor of 1.8 than those calculated here for $\epsilon=3.0$.

A further approximation is that of using free-ion wave functions for the crystal core states with no corrections for the crystal field or the overlapping of core states. It is difficult to estimate the effects of these approximations since there have been few studies of wave functions of ions in crystals. To a first approximation the negative ions are in a crystal field potential well similar to that for an F center. This tends to bind the electrons more tightly and there is a marked contraction of the tail of the Cl^- wave function.[49,50] This contraction tends to decrease the overlap integrals, but it is partially offset by the increase in spin-orbit interaction of the more compact wave function. The alkali ions experience a similar potential, but with the opposite sign so that the valence functions tend to expand. However, the positive ions are small and are almost completely contained within a relatively constant portion of the point-ion potential. If only the spherically symmetric component of the point-ion crystal field is considered, there is almost no difference between the free ion and the crystal wave functions for positive ions.[50]

The effect of neglecting overlap between core functions centered on different ions has been investigated in several simple cases involving clusters of 4–6 ions. For typical valence-valence overlap

TABLE III. Calculated spin-orbit configuration interaction parameters $\zeta_{2p,np}=2\langle\phi_{2p}^{3/2,3/2}|\, h_{so}\,|\phi_{np}^{3/2,3/2}\rangle$ for several states of the F center in RbCl.

Electronic state	$\zeta_{2p,np}$ (meV)
$3p$	−4.79
$4p$	−0.97
$5p$	−0.17
$6p$	−0.02

integrals of the order of 0.1, neglecting core-core overlap was found to lead to an overestimate of $\sum_\alpha S_{i,\alpha} S_{\alpha,j}$ by roughly 15% if the sum over ϵ was limited to valence functions. On the other hand, the deep-lying core states which have little overlap with one another contribute to both $\sum_\alpha S_{i,\alpha} S_{\alpha,j}$ and $\langle \phi_i | h_{so} | \phi_j \rangle$, so that the error in these matrix elements is probably less than 15%.

In addition to uncertainties in the wave functions, the positions of the ions neighboring the F center are not well known. For simplicity they have been chosen to be at the normal lattice sites for a perfect crystal. However, the errors introduced by this choice are probably less than 10% because the total spin-orbit interaction is rather insensitive to the exact positions of the nearest-neighbor ions.

Considering all the approximations and the numerical methods involved, a reasonable estimate is that the calculated spin-orbit interactions are probably good to a factor of 2.

IV. PHYSICAL PICTURE OF VARIATION OF SPIN-ORBIT SPLITTING WITH N

The physical picture behind the large negative spin-orbit splitting of the F band was developed in detail in Ref. 34. The essence of the argument is that the F-center wave functions must have a number of loops and nodes in the vicinity of the ionic nuclei to ensure their orthogonality to the occupied core states and the correct behavior near the nuclei.[51] This structure corresponds to a nonzero angular-momentum state as viewed from the ionic nuclei where the spin-orbit interaction is large. In the case of the $2p$ state this local angular momentum is, on the average, opposite in direction to that of the total wave function as viewed from the center of the vacancy. This locally negative angular momentum yields the negative spin-orbit splitting.

In the present paper we have to consider how the spin-orbit splitting changes with state of excitation. The detailed numerical results show that two effects are involved: (a) the change in F-center wave-function amplitude near the ions and (b) the oscillations of the wave functions in the higher excited states.

To understand the first of these it is useful to consider initially the term $\sum_\alpha S_{i,\alpha}^2$ in the normalization. This sum is a measure of the amount of F-center state in the neighborhood of the ions and —unlike the spin-orbit interaction—it decreases by only 6% on going from the $2p$ to the $3p$ state even though the maximum in the electronic charge density moves from $\sim 7.4a_0$ to $\sim 29a_0$ (see Fig. 2). The reason for this approximately constant overlap for two states with spin-orbit interaction differing by a factor of 5 is that the predominant contributor to the overlap sum is overlap with S-like core states, whereas the spin-orbit interaction arises primarily from overlap with P-like cores.

The overlap with S-like core states is determined by the local S-like component of the F-center-model wave function $u_i(\vec{r})$. This is roughly a measure of the amplitude of $u_i(\vec{r})$ at the nucleus of the ion in question, so that the overlaps are proportional to $V^{-1/2}$, where V is a measure of the volume occupied by the F-center electron. The number of terms involved in a summation over all the overlapped ions is itself proportional to V, so the portion of $\sum_\alpha S_{i,\alpha}^2$ arising from S overlaps is independent of the extent of the wave function.

Now, the spin-orbit interaction arises from the presence locally of nonzero angular-momentum components of the F-center wave function $u_i(\vec{r})$ near the host lattice ions. In the present case the major contributors are the P-like components. Unlike the S-core-state overlaps, the overlap with P-core states falls off faster than $V^{-1/2}$, so that summations quadratic in P-function overlaps can be expected to decrease as the electronic state becomes more diffuse. Qualitatively this can be seen by noting that the P-like character of the unorthogonalized model wave function $u_i(\vec{r})$ is proportional to the gradient of $u_i(\vec{r})$ at the point in question. Thus, a summation in the squares of P overlaps is proportional to a summation of the square of the gradients of $u_i(\vec{r})$ and, hence, is very crudely related to the kinetic energy of the state in question. The latter decreases in going from one bound state to a higher one, so that a similar decrease is expected in the spin-orbit interaction. In the present calculation the decrease in the spin-orbit interaction arising from the decrease in the local P-like character of $u_i(\vec{r})$ was estimated by summing the contributions to the $3p$-state spin-orbit splitting from the various shells of ions without regard to sign and comparing this with the $2p$-states splitting. It was found that $\sim 40.6\%$ of the total decrease in spin-orbit splitting arises from the decreased P-like character in $u_{3p}(\vec{r})$.

The remaining 59.4% of the decrease in spin-orbit interaction results from the oscillations of the $3p$ state and the resultant alternation in the sign of the individual ionic contributions as a function of the ion's distance from the center of the vacancy. This is illustrated in Fig. 3, which shows the radial part of the $3p$ wave function and the average per-ion spin-orbit contribution of a Cl^- ion as a function of its position. It is evident that the single oscillation of the $3p$ wave function results in several oscillations of the ionic contribution to the spin-orbit splitting.

The details of this are most easily seen for the ion-ion contribution to the spin-orbit interaction Eqs. (11) and (12). Since the p-σ overlaps are generally larger than the corresponding p-π overlaps and both are much larger than D-core overlaps, the major contribution to the spin-orbit interaction is from the terms in Eq. (11) involving

TABLE IV. Calculated normalization and spin-orbit interaction matrix elements for the RbCl F center. Energies are given in units of 10^{-3} eV.

	$2p$ state $n=m=2$	$3p$ state $n=m=3$	$2p$-$3p$ configuration interaction $n=2$, $m=3$
Normalization N_{np}	1.48	1.43	...
Overlap $\langle\phi_{np}\mid\phi_{mp}^{(1)}\rangle$	...	...	−0.01
$\langle\phi_{np}^{3/2,3/2}\mid h_{so}\mid\phi_{mp}^{3/2,3/2}\rangle/N_{np}N_{mp}$:			
Ion-ion terms	−2.33(3)	−0.509(5)	−1.11(2)
Vacancy-ion cross terms	+0.002	+0.0008	+0.001
Vacancy-centered terms	−0.001	−0.0001	−0.0005
Total	−2.33	−0.510	−1.11
Total corrected for np-mp overlap	...	−0.533	−1.14

$S_\sigma S_\pi$. Very roughly, the σ-like overlaps are proportional to the radial derivative of the model wave function $\partial u_i/\partial r$ [see Eq. (13)], and the π-like overlap is similarly related to the azimuthal derivative $\partial u_i/\partial\theta$, which has the same sign as the function itself. These derivatives have oscillations that are out of phase, so that their product $S_\sigma S_\pi$ displays a number of damped oscillations. These oscillations are indicated in Fig. 3, where the axis is divided into four regions. In the first region (which is within the vacancy) both $\partial u/\partial r$ and $\partial u/\partial\theta$ are positive and, were there ions here, they would yield a positive spin-orbit interaction. In the second region, $\partial u/\partial r$ is negative, but $\partial u/\partial\theta$ is positive, yielding a negative contribution to the spin-orbit interaction. In the third region both derivatives are negative and the spin-orbit contribution is positive, while in the fourth region the derivatives

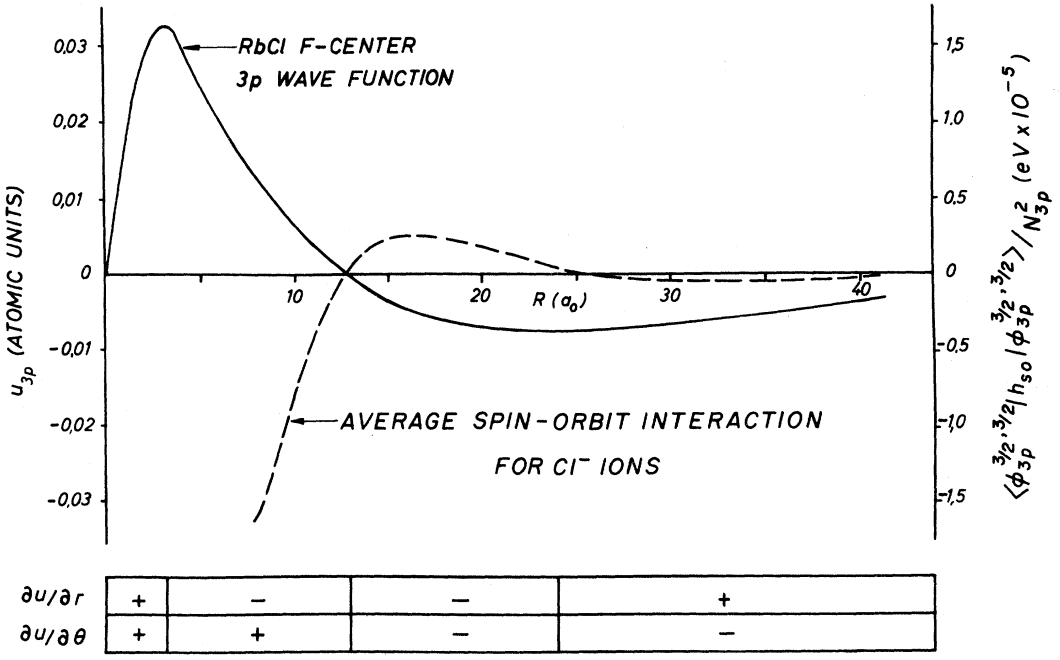

FIG. 3. Relation of the spin-orbit interaction in the $3p$ state to the model wave function. The major contribution to the spin-orbit interaction arises from the ion-ion term involving the product of σ and π overlap integrals for P-like core states. The σ overlap is roughly proportional to the radial derivative of the F-center function $\partial u/\partial r$, and the π overlap is similarly related to the azimuthal derivative $\partial u/\partial\theta$. As explained in the text, the $3p$ model wave function may be divided into four regions for different combinations of the signs of these derivatives. The sign of the spin-orbit interaction then alternates from region to region.

have opposite signs, giving a negative spin-orbit contribution again. Of course, there is some departure of the sign of the total spin-orbit interaction from this simplified picture at the borders of the regions because we have considered only the $S_\sigma S_\tau$ terms in this qualitative discussion. However, the calculations show that the neglected terms give only slight corrections to the argument.

In the case of the $2p$-np matrix elements the effect of the decrease in local density of the np state becomes much more important. In these matrix elements the $2p$ part remains the same, but the np part becomes more diffuse as n increases. Thus, there is a rapid decrease in the joint amplitude of the $2p$ and np functions at the surrounding nuclei and consequently a decrease in the matrix element. In addition, as with the diagonal matrix elements, the np state oscillates more with higher n, giving rise to regions of spin-orbit contributions with alternating sign that further decrease the matrix elements. Since the decrease in the product of $2p$ and np functions is quite rapid, the off-diagonal terms decrease much faster with n than do the diagonal terms. This can be seen by a comparison of Tables II and III or Eqs. (20) and (21).

V. COMPARISON OF THEORY WITH EXPERIMENT

A. Moments Analysis and Overlapping Absorption Bands

Magneto-optic experiments carried out in the Faraday orientation provide a direct measurement of the F- and K-band spin-orbit interaction. Since the K band appears to be a composite band, the calculated splittings cannot be compared directly with experiment; rather, a weighted average must be used. In the present section we consider how these averages should be taken.

In the magneto-optic experiments of interest here the dichroism of circularly polarized light or the Faraday rotation of linear light is measured for propagation parallel to the magnetic field.[1-10] These measurements are most profitably analyzed in terms of the change in moments[12,13] of the absorption bands with magnetic field and spin polarization. For the present discussion it is sufficient to consider the zeroth- and first-moment changes.

The zeroth moment, or area under an absorption band's line-shape function,[52] is a measure of the probability of the transition(s) involved. It may be varied by an external perturbation which mixes nearby configurations (with differing absorption strengths) into the state(s) for the transition in question. In the allowed K-band model adopted here, the orbit-Zeeman and spin-orbit interactions have off-diagonal matrix elements connecting the Γ_4^- levels responsible for the F and K bands. Consequently, an exchange in area between the two bands occurs when an external magnetic field is applied and whenever the electron spins are polarized.

A straightforward calculation[18,50] of the change in zeroth moment of transitions to the np state taking into account mixing with the $2p$ F-band state to first order yields

$$\left.\frac{\Delta A_n}{A_n}\right|_{r/l} = \mp \frac{2}{E_{np} - E_{2p}} \left(\frac{A_F}{A_n}\right)^{1/2} \times (\mu_B H \langle \phi_{2p}^{3/2,3/2} | L_z | \phi_{np}^{3/2,3/2} \rangle + \zeta_{2p,np} \langle S_z \rangle) \ . \quad (30)$$

Here E_{np} is the energy of the np state, and A_F and A_n are the zeroth moments of the F ("$1s \rightarrow 2p$") band and the np K-band component ("$1s \rightarrow np$"), respectively. The quantity $\langle S_z \rangle$ is the thermal average of the z component of electron spin in the ground $\Gamma_1^+(1s)$ state. The subscript r/l and the sign $\mp$ indicate that the negative sign is to be associated with right-hand circularly polarized light and the positive sign with left-hand circularly polarized light.[53] ΔA_n consists of two parts: a diamagnetic (temperature-independent) change arising from orbit-Zeeman configuration mixing and a paramagnetic (temperature-dependent) part which depends on the spin-orbit interaction and the spin polarization.

The change $\Delta\langle E \rangle$ in first moment—or average energy—may be calculated in similar fashion. To lowest order it is not affected by configuration interaction and the result is the well-known relation[12,13,53]

$$\Delta \langle E_n \rangle_{r/l} = \mp (g_{\rm orb} \mu_B H + \tfrac{2}{3} \Delta_{np} \langle S_z \rangle) \ , \quad (31)$$

where Δ_{np} is the spin-orbit splitting of the nth p level and

$$g_{\rm orb} = \langle \phi_{np}^{3/2,3/2} | L_z | \phi_{np}^{3/2,3/2} \rangle \ . \quad (32)$$

Again there are two terms in the moment charge: a temperature-independent diamagnetic term arising from the orbit-Zeeman interaction and a temperature-dependent paramagnetic contribution from the spin-orbit interaction. Because we are concerned with spin-orbit matrix elements, we shall limit discussion to the paramagnetic terms in what follows.

In the many-P-state model the observable F-K configuration interaction matrix element and the K-band spin-orbit splitting are averages over the whole K band. To derive these average values we note that in the many-P-state model the area A_N of a band involving transitions to the $3p$, $4p$, ..., Np states is given by

$$A_N = \sum_{n \geq 3}^{N} A_n \ , \quad (33)$$

where A_n is the area of the band resulting from the np state. Then using the expression for $\Delta A/A$

of an allowed transition, Eq. (30), we have for the paramagnetic part

$$\frac{1}{\langle S_z\rangle}\frac{\Delta A_N}{A_N}\bigg|_{r/l}^{\text{para}} = \mp\frac{2}{E_N - E_F}\left(\frac{A_F}{A_N}\right)^{1/2}\zeta_{F,N}\ , \tag{34}$$

where E_N is the average energy of the composite band and the average spin-orbit matrix element is given by

$$\zeta_{F,N} = 2\sum_{n\geq 3}^{N}\frac{E_N - E_F}{E_n - E_F}\left(\frac{A_n}{A_N}\right)^{1/2} \times\langle\phi_{2p}^{3/2,3/2}|h_{so}|\phi_{np}^{3/2,3/2}\rangle$$

$$= \sum_{n\geq 3}^{N}\frac{E_N - E_F}{E_n - E_F}\left(\frac{A_n}{A_N}\right)^{1/2}\zeta_{2p,np}\ . \tag{35}$$

The first moment of the composite band, $\langle E_N\rangle$, is

$$\langle E_N\rangle = \sum_{n\geq 3}^{N}\langle E_n\rangle\frac{A_n}{A_N}\ , \tag{36}$$

so that

$$\Delta\langle E_N\rangle = \sum_{n\geq 3}^{N}\Delta\langle E_n\rangle\left(\frac{A_n}{A_N}\right) + \sum_{n,n'\geq 3}^{N}\frac{(E_n - E_{n'})\Delta A_n A_{n'}}{A_N^2}\ . \tag{37}$$

Now, Eq. (37) may be divided into its paramagnetic (temperature-dependent) and diamagnetic (temperature-independent) parts. The paramagnetic part, which is of interest here, may be simplified by using the experimental observation[15] that the change in absorption is approximately proportional to the absorption at low temperatures where paramagnetic terms dominate. This will hold for the composite band provided that $(\Delta A_n)_{\text{para}} \approx cA_n$, where c is the same constant for all n. In this case the double sum in the second term of Eq. (37) consists of pairs of terms having opposite sign which cancel, leaving just the first term involving $\Delta\langle E_n\rangle$. Then, from the expression for $\Delta\langle E_N\rangle$ for allowed transitions, we have for the paramagnetic change in first moment,

$$(1/\langle S_z\rangle)\Delta\langle E_N\rangle\big|_{r/l}^{\text{para}} = \mp\tfrac{2}{3}\Delta_N\ , \tag{38}$$

where

$$\Delta_N = \sum_{n\geq 3}^{N}\Delta_n\left(\frac{A_n}{A_N}\right)\ . \tag{39}$$

In the present work the values of $\zeta_{F,K}$ and Δ_K were evaluated by approximating A_n/A_K by the ratio of the oscillator strength of the transition involved to that of the K band as calculated from Eq. (33). Numerical values were taken from Ref. 20 and as an example the ratios for $N=\infty$ are summarized in the third column of Table II.

A point that is often glossed over in discussion of relations like Eqs. (30) and (34) connecting off-diagonal matrix elements with zero moment changes is the question of the phase of off-diagonal matrix elements. Since the phases of the various state functions involved are arbitrary, the off-diagonal matrix elements have arbitrary nonzero phase factors. These phases, of course, are not observable, but an uncritical examination of Eqs. (30) and (34) makes it appear that they can be determined. The explanation is that a choice of phase has tacitly been assumed in deriving the formula for the change in area of allowed transitions. This choice is implicit in the replacement of the ratio of dipole matrix elements for transitions from the ground state to the excited states under consideration by the positive radical $(A_{2p}/A_{np})^{1/2}$, where A_{2p} and A_{np} are the areas of the shape functions for transitions to state φ_{2p} and state φ_{np}, respectively.

This replacement is valid *if* the two dipole transition matrix elements have the same phase. In the case we are concerned with, the transition matrix elements are determined mainly by the regions of the excited states within the first node.[54] Thus for Eqs. (30) and (34) to hold, we must require that ϕ_{2p} and ϕ_{np} have the same phase in the region near the origin. In the present calculation the conventional choice of real radial wave functions with a positive loop between the origin and the first node has been made to satisfy this condition. Hence, within our choice of phase, the sign of the off-diagonal matrix element is meaningful.

B. Current Experimental Situation and Comparison with Theory

a. F-band spin-orbit splittings. The spin-orbit splitting of the F band, Δ_F, in RbCl has been measured by Gareyte and d'Aubigné,[5] d'Aubigné,[55] and Brown *et al.*[8,56] Moments analysis of both Faraday rotation and circular dichroism data yields values for Δ_F ranging from -15×10^{-3} to -17×10^{-3} eV. They are listed in Table V together with the predicted splitting of -15.3×10^{-3} eV. The agreement between theory and experiment is embarrassingly good, especially for the Faraday rotation data of Brown *et al.*

b. K-band spin-orbit splitting. A first moment change in the K band was originally observed by Brown, Cavenett, and Hayes[16] in Faraday rotation studies. They found a weak rotation at the position of the K band in colored RbCl which was about 80 times smaller than the F-band rotation. In the approximation of a rigid shift of the band the magnitude of the first moment change may be estimated from the observed rotation, the F-band splitting, and the line shapes via the formalism of Mort *et al.*[6] [especially their Eq. (10)]. This yields an approximate K-band splitting Δ_K of -3.6×10^{-3} eV in RbCl. Circular dichroism measurements allow a very much better separation of the magneto-optic effects of the F and K bands. Using this technique,

TABLE V. Observed and predicted F- and K-band splittings for the F center in RbCl. The splitting Δ is the energy difference between the $\Gamma_8^-(P_{3/2})$ and the $\Gamma_6^-(P_{1/2})$ states and is given in units of 10^{-3} eV. The negative sign indicates that the Γ_6^- state lies above the Γ_8^- state. Predicted average splittings are given for several possible composite K bands involving np states with $n \geq 3$; for details see Sec. V. The abreviations MCD and FR stand for magnetic circular dichroism and Faraday rotation, respectively.

	Experiment		Theory	
Band	Δ (meV)	Method	States	Δ (meV)
F[a]	-17.3[b]	MCD		
	-15.1[c]	FR	$2p$	-15.3
	-17.1[c]	MCD		
K (entire band)	-3.6[d]	FR	$3p$	-3.2
K_1 (subband)	-3.9[e]	MCD	$3p+4p$	-2.8[f]
			$3p+4p+5p$	-2.6[f]
			$\sum_{n\geq 3} np$	-2.2[f]

[a]Early reports of splittings of ~ -24 eV (Ref. 5) were based on a rigid-shift analysis of data which was later shown to be inappropriate. These numbers have consequently been omitted in this table.

[b]Y. M. d'Aubigné, Ref. 55.

[c]F. C. Brown *et al.*, Refs. 8 and 56.

[d]The author's approximate analysis of data of F. C. Brown *et al.*, Ref. 16.

[e]E. Krätzig and W. Staude, Ref. 18.

[f]Weighted averages calculated from Eq. (39).

Krätzig and Staude[17,18] have measured both the zeroth and first moment changes in the K band. These authors report a splitting of the K_1 subband in RbCl of -3.9×10^{-3} eV.[18] The splitting of the K_2 band was too small to be measured.

It should be noted that these measured splittings are less than would be expected on an alkali-atom model. For comparison Brown *et al.*[16] estimated that the K-band Faraday rotation would be $\frac{1}{65}$ of that of the F band for an atomic n^{-3} dependence on principal quantum number; experimentally the observed rotation is less by a factor of $\frac{1}{80}$.

Several calculated values for the K-band spin-orbit splitting are given. They are the splitting of the $3p$ state Δ_{3p} and the weighted averages for composite bands involving transitions to $3p$ and $4p$ states, to $3p$, $4p$, and $5p$ states, and to all bound np states for $n \geq 3$. The agreement is good, especially if the K_1 band is associated with transitions to the first few excited states for $n \geq 3$.

c. F-K configuration interaction. The change in area of the K band resulting from mixture with F-band states by magnetic perturbations has been investigated in a number of salts by d'Aubigné and Gareyte[15] and by Krätzig and Staude.[18] For reference all their published results are compared in Table VI; here both $\langle S_z \rangle^{-1} (\Delta A_K / A_K)_r^{\text{para}}$ and the derived off-diagonal matrix elements are given. Krätzig and Staude do not report the zeroth moment change itself, but rather derived quantities related to the off-diagonal orbit-Zeeman and spin-orbit matrix elements. However, for comparison with d'Aubigné and Gareyte's results we have chosen to use their analysis in reverse and have calculated back to the observed area change. The agreement between the two sets of experiments is quite good, especially for RbCl.

TABLE VI. Observed paramagnetic zeroth moment changes for right-hand circular-polarized light and the derived F-K spin-orbit configuration mixing parameters. Energies are given in units of 10^{-3} eV.

	d'Aubigné and Gareyte		Krätzig and Staude	
Salt	$\frac{1}{\langle S_z \rangle} \frac{\Delta A_K}{A_K}\Big\|_r^{\text{para}}$	ζ_{FK}[a] (meV)	$\frac{1}{\langle S_z \rangle} \frac{A_K}{A_K}\Big\|_r^{\text{para}}$	ζ_{FK}[b] (meV)
KCl	0.026	-1.9	0.039	-1.8
KBr	···	···	0.113	-4.6
KI	···	···	0.134	-3.5
RbCl	0.106	-5.6[c]	0.106	-4.2[c]
RbBr	0.174	-12.0	0.152	-6.8
RbI	···	···	0.322	-10

[a]Calculated from Eq. (34) using F- and K-band areas and energies given by Lüty, Ref. 19.

[b]Calculated from $\zeta_{FK} = \lambda_{FK} \langle y_K | L_z | x_F \rangle$ in the notation of Ref. 18. See Refs. 18 and 46.

[c]Although the zeroth-moment change for RbCl is the same for both sets of experiments, the values of ζ_{FK} differ slightly because of minor differences in K- band area and energies given in Refs. 18 and 19.

Theoretical values for the spin-orbit parameter are given in Table VII. The values are based on assumption of K-band transitions to just the $3p$ level, and composite bands involving the $3p$ and $4p$ states, the $3p$, $4p$, and $5p$ states, and all bound np states for $n \geq 3$. Again, the agreement is good,

TABLE VII. Observed and predicted F-K spin-orbit configuration mixing parameters ζ_{FK} for RbCl. Energies are given in units of 10^{-3} eV. Average values of ζ_{FK} are given for several possible composite K bands involving np states for $n \geq 3$; for details see Sec. V.

Experiment	Theory	
ζ_{FK} (meV)	States in K band	ζ_{FK} (meV)
-5.6[a]	$3p$	-4.8
	$3p+4p$	-4.4[b]
-4.2[c]	$3p+4p+5p$	-4.1[b]
	$\sum_{n=3}^{\infty} np$	-3.8[b]

[a]From d'Aubigné and Gareyte, Ref. 15, using F- and K-band areas and energies given by Lüty, Ref. 19.

[b]Weighted averages calculated from Eq. (35).

[c]From Krätzig and Staude, Ref. 18.

TABLE VIII. Relative contributions of positive and negative ions to the F-center spin-orbit interaction in NaCl and RbCl. Types I and II refer to Gourary and Adrian's designation of trial functions (see Ref. 57).

Material	Matrix element	Positive ion (%)	Negative ion (%)
NaCl	$2p$ diagonal (type I)	4.5	95.5
NaCl	$2p$ diagonal (type II)	7.3	92.7
RbCl	$2p$ diagonal	60.3	39.7
RbCl	$3p$ diagonal	68.5	31.5
RbCl	$2p$-$3p$ off diagonal	64.1	35.9

especially if the K_1 band is identified with transitions to the $3p$ state and perhaps the next few higher-energy P states.

C. Comments and Conclusion

In Table VIII the relative contributions of cations and anions to the F-center spin-orbit matrix elements in RbCl found in the present calculation are compared with the values found previously for NaCl. The striking difference between the two salts is that in NaCl the Na^+ ion contributes less than 8% of the spin-orbit interaction, whereas in RbCl the Rb^- ion contributes over 60%. This difference reinforces the conclusion drawn in Ref. 34 that in the salts of the light alkalis the halide ion, though not the nearest neighbor, dominates the spin-orbit splitting because its wave functions are diffuse and lead to large overlap integrals. Only for the heaviest alkali ions does the effect of a large nuclear charge overcome that of the smaller overlaps to allow the alkali ion to make an important contribution to the total spin-orbit interaction.

In the case of the experimental K-band parameters it should be stressed that the data have been treated within the framework of the rigid-shift approximation. This holds both in the work of Krätzig and Staude[17,18] and in the present author's rough analysis of the K-band Faraday rotation data of Brown *et al.*[16] In the original estimates of F-band splittings[6] in RbCl the rigid-shift approximation led to overestimates by a factor of ~1.6–1.8. A similar overestimate in the rigid-shift values of Δ_K cannot be excluded. Furthermore, since the shifts are most pronounced near the peak of the K band, contributions from the tail may have been neglected to some extent in experiments in which the separation into K_1 and K_2 bands was not made. This would tend to emphasize the lower excited states and consequently overestimate the experimental quantities for the composite band.

In comparing the calculated and experimental values it must also be borne in mind that the estimates in Sec. VI indicate that the predicted values are probably good to somewhat better than a factor of 2. Considering this, the agreement between theory and experiment is far better than would be expected *a priori* and is easily within both calculational and experimental error. Thus, the allowed-transition model of the K band correctly predicts the band's observed magneto-optic parameters. This, together with the conclusions drawn from stress experiments,[11,27] strongly supports the Mott-Gurney[22] assignment of the K band to allowed transitions of the F center to a series of bound excited states lying above the bound state responsible for the F band.

ACKNOWLEDGMENTS

The author is indebted to Professor F. C. Brown, Dr. Y. M. d'Aubigné, Dr. E. Krätzig, and Dr. W. Staude for keeping him informed of the results of their K-band studies and for stimulating discussions and communications. Particular thanks are due to Professor H. Pick for his encouragement and for making available to the author the facilities of the II. Physikalisches Institut der Universität Stuttgart, where a portion of this work was completed. The aid of I. Straubenmüller and Fr. Schiel in preparing part of the manuscript is gratefully acknowledged.

APPENDIX A: EVALUATION OF LATTICE SUMS FOR NaCl-TYPE LATTICE

The expressions for the normalization and the spin-orbit matrix elements involve lattice sums of the form $\sum_\alpha S_{i,\alpha}S_{\alpha,j}$, $\sum_{\alpha,\beta} S_{i,\alpha}S_{\beta,j}\langle\varphi_\alpha|h_{so}|\varphi_\beta\rangle$, and $\sum_\alpha S_{i,\alpha}\langle\varphi_\alpha|h_{so}|u_j\rangle$, where the sums over α and β run over all occupied core states. In the case of centers with high symmetry, these sums may be reduced from a sum over all ions to a sum over shells of ions in which the terms are independent of the specific arrangement of the ions within the shells. As an example of this reduction consider $\sum_\alpha S_{i,\alpha}S_{\alpha,j}$ for the particular case of u a Γ_4^- function transforming like $\mathcal{R}(r)\,x/r$. We treat separately the S-, P-, and D-like core states of an ion located at the general point (X_I, Y_I, Z_I) on the shell of radius $R=(X_I^2+Y_I^2+Z_I^2)^{1/2}$.

The overlap of u_i with an S-like ion state $\varphi_{\alpha S}$ is[38]

$$S_{ix,s\alpha}=\langle u_{ix}|\,\varphi_{\alpha S}\rangle = l_I S(p_i, s_\alpha\sigma)\,, \tag{A1}$$

where $l_I = X_I/R$ is the x-direction cosine of the ion and $S(p_i, s_\alpha\sigma)$ is the overlap of the vacancy-centered P-like function with the S-like core function $\varphi_{\alpha S}$. Then the sum of the squares of the overlaps in the shell is

$$\sum_\alpha{}' S_{i,\alpha}S_{\alpha,j} = \sum_{\alpha I}{}' l_I^2 S(p_i, s_\alpha\sigma)\,S(p_j, s_\alpha\sigma)$$
$$= \tfrac{1}{3}n\sum_\alpha{}'' S(p_i, s_\alpha\sigma)\,S(p_j, s_\alpha\sigma)\,. \tag{A2}$$

Here we have used the fact that in the NaCl lattice

the n ions in the shell lie at points that are permutations of the triplet $[X_I, Y_I, Z_I]$ so that $\frac{1}{3}n$ have $l_I = \pm X_I/R$, $\frac{1}{3}n$ have $l_I = \pm Y_I/R$, and $\frac{1}{3}n$ have $l_I = \pm Z_I/R$.

For the three P-like core states transforming like x, y, and z the overlaps of an x-like F-center function are

$$\begin{aligned}
\langle u_{ix} | \varphi_{\alpha px}\rangle &= l_I^2 S(p_i, p_\alpha\sigma) + (1 - l_I^2) S(p_i, p_\alpha\pi),\\
\langle u_{ix} | \varphi_{\alpha py}\rangle &= l_I m_I S(p_i, p_\alpha\sigma) - l_I m_I S(p_i, p_\alpha\pi), \qquad \text{(A3)}\\
\langle u_{ix} | \varphi_{\alpha pz}\rangle &= l_I n_I S(p_i, p_\alpha\sigma) - l_I n_I S(p_i, p_\alpha\pi),
\end{aligned}$$

where $S(p_i, p_\alpha\sigma)$ and $S(p_i, p_\alpha\pi)$ are the σ and π overlaps of a P-like function centered on the vacancy and the P-like core functions $\varphi_{\alpha P}$. Here l_I, m_I, and n_I are the direction cosines of the Ith ion relative to the center of the vacancy. Summing these products over the ions in a single shell yields

$$\begin{aligned}
\sum{}' S_{i,\alpha} S_{\alpha,j} &= \sum_{\alpha,I}{}' [l_I^2 S(p_i, p_\alpha\sigma) S(p_j, p_\alpha\sigma)\\
&\quad + (1 - l_I^2) S(p_i, p_\alpha\pi) S(p_j, p_\alpha\pi)]\\
&= \tfrac{1}{3}n \sum_\alpha{}'' [S(p_i, p_\alpha\sigma) S(p_j, p_\alpha\sigma)\\
&\quad + 2S(p_i, p_\alpha\pi) S(p_j, p_\alpha\pi)]. \qquad \text{(A4)}
\end{aligned}$$

Using the equations given in Ref. 38 for D-function overlaps yields a similar result for the D-core states, but with $S(p_i, p_\alpha\sigma)$ and $S(p_i, p_\alpha\pi)$ replaced by the D-like σ and π overlaps $S(p_i, d_\alpha\sigma)$ and $S(p_i, d_\alpha\pi)$.

For convenience we have considered only an F-center function transforming like x; however, by symmetry these results also hold for the functions transforming like y and z. Furthermore, they hold for any linear combination of these functions. This is generally true, since cross terms of the form $\sum_\alpha S_{ix,\alpha} S_{\alpha,jy}$ are zero. For example, in the case of S-core states of ions in a single shell this cross term is

$$\sum_\alpha{}' S_{ix,\alpha} S_{\alpha,jy} = \sum_{\alpha,I} l_I m_I S(p_i, s_\alpha\sigma) S(p_j, s_\alpha\sigma), \qquad \text{(A5)}$$

but in the NaCl structure the product of direction cosines $l_I m_I$ sums to zero. Similar arguments hold for overlap with other symmetry core states.

APPENDIX B: EVALUATION OF SPIN-ORBIT INTEGRALS

In Ref. 34 the method of calculating the spin-orbit interaction was outlined; however, several questions have arisen concerning the details of evaluating the integrals involved. Both the overlap and spin-orbit elements may be evaluated readily by the "α-function" expansion technique of Löwdin.[58] As an example of this we consider the terms in the expression for the spin-orbit elements in the particularly simple case where the u's transform like a $J = \frac{3}{2}$, $m_J = \frac{3}{2}$ state. From Eq. (4) we have

$$\langle \phi_i | h_{so} | \phi_j \rangle = \epsilon_1 + \epsilon_2 + \epsilon_3, \qquad \text{(B1)}$$

where

$$\epsilon_1 = N_i N_j \langle u_i | h_{so} | u_j \rangle, \qquad \text{(B2)}$$

$$\begin{aligned}
\epsilon_2 = -N_i N_j \Big(&\sum_\alpha S_{i,\alpha} \langle \varphi_\alpha | h_{so} | u_j \rangle\\
&+ \sum_\beta S_{\beta,j} \langle u_i | h_{so} | \varphi_\beta \rangle \Big), \qquad \text{(B3)}
\end{aligned}$$

and

$$\epsilon_3 = N_i N_j \sum_{\alpha,\beta} S_{i,\alpha} S_{\beta,j} \langle \varphi_\alpha | h_{so} | \varphi_\beta \rangle. \qquad \text{(B4)}$$

We shall treat these terms separately and for simplicity limit consideration to the ions in a single shell of radius R with ions at (X_I, Y_I, Z_I).

Consider the special case of a vacancy-centered function transforming like Y_1^1 and with spin-up,

$$u_i = \mathcal{R}_i(r)\, Y_1^1 \uparrow = (3/8\pi)^{1/2} \mathcal{R}_i(r) [(x + iy)/r] \uparrow, \qquad \text{(B5)}$$

where $\uparrow$ is the spin-up spinner. Using the differential form of $\vec{L}_I$ of Eq. (3) yields

$$\begin{aligned}
\langle u_i | h_{so} | u_j \rangle = (3/16\pi)\hbar^2 \textstyle\sum_I \int &\mathcal{R}_i(r) \mathcal{R}_j(r) \xi(r_I)\\
&\times [(x_I^2 + y_I^2 + x_I X_I + y_I Y_I)/r^2] d^3r. \qquad \text{(B6)}
\end{aligned}$$

Here the coordinates x_I are measured from the ion, i.e., $\vec{r}_I = \vec{r} - \vec{R}_I$, etc. Equation (B6) may be written in terms of real spherical harmonics[58] as

$$\begin{aligned}
\langle u_i | h_{so} | u_j \rangle = \hbar^2 \textstyle\sum_I \{ &\tfrac{1}{2} \int [r^{-2} \mathcal{R}_i(r) \mathcal{R}_j(r)\, Y_{0,0}(\vec{r})][r_I^2 \xi(r_I) Y_{0,0}(\vec{r}_I)] d^3r\\
&- (1/2\sqrt{5}) \int [r^{-2} \mathcal{R}_i(r) \mathcal{R}_j(r)\, Y_{0,0}(\vec{r})][r_I^2 \xi(r_I)\, Y_{2,0}(\vec{r}_I)] d^3r + \tfrac{1}{4}\sqrt{3} X_I \int [r^{-2} \mathcal{R}_i(r) \mathcal{R}_j(r) Y_{0,0}(\vec{r})]\\
&\times [r_I \xi(r_I) Y_{1,1}(\vec{r}_I)] d^3r + \tfrac{1}{4}\sqrt{3} Y_I \int [r^{-2} \mathcal{R}_i(r) \mathcal{R}_j(r) Y_{0,0}(\vec{r})][r_I \xi(r_I) Y_{1,\bar{1}}(\vec{r}_I)] d^3r \}. \qquad \text{(B7)}
\end{aligned}$$

Here $Y_{L,M}(\vec{r})$ denote the real spherical harmonics involving $\sin M\phi$, and $Y_{L,\bar{M}}(\vec{r})$ are the harmonics involving $\cos M\phi$. The integrals are now in the form of a spherically symmetric function centered on the vacancy times a function centered on the Ith ion transforming like $Y_{L,M}$. Since the function

centered on the ion involves $\xi(r_I)$, which behaves like r_I^3 near the nucleus, it is convenient to take the ion nucleus as the origin of coordinates and express $r^{-2}\mathcal{R}_i(r)\mathcal{R}_j(r)Y_{0,0}(\vec{r})$ in an α-function expansion about this point. This choice leads to an additional factor of r_I^2 in the integrand from the volume element and thus avoids integration over a singularity.

As in Appendix A, the individual integrals may be most conveniently expressed in terms of the direction cosines of the ion involved and integrals dependent only on the shell radius. This yields

$$\langle u_i | h_{so} | u_j \rangle = \sum_I \{\lambda_{ss} - (1/\sqrt{5})[n_I^2 - \tfrac{1}{2}(l_I^2 + m_I^2)]\,\lambda_{sd\sigma} + \tfrac{1}{2}\sqrt{3}(l_I^2 + m_I^2)R\lambda_{sp\sigma}\} \quad , \tag{B8}$$

where the λ's are given by

$$\lambda_{ss} = \tfrac{1}{2}\hbar^2 \int [r^{-2}\mathcal{R}_i(r)\mathcal{R}_j(r)Y_{0,0}(\vec{r})][r^2\xi(r)Y_{0,0}(\vec{r})]\,d^3r \ , \tag{B9}$$

$$\lambda_{sd\sigma} = \tfrac{1}{2}\hbar^2 \int [r^{-2}\mathcal{R}_i(r)\mathcal{R}_j(r)Y_{0,0}(\vec{r})][r^2\xi(r)Y_{2,0}(\vec{r})]\,d^3r \ , \tag{B10}$$

$$\lambda_{sp\sigma} = \tfrac{1}{2}\hbar^2 \int [r^{-2}\mathcal{R}_i(r)\mathcal{R}_j(r)Y_{0,0}(\vec{r})][r\xi(r)Y_{1,0}(\vec{r})]\,d^3r \ . \tag{B11}$$

For ease in applying Löwdin's expansion techniques these integrals are to be evaluated for an ion on the z axis, that is, with $\vec{r} = x\hat{i} + y\hat{j} + (z - R)\hat{k}$. Summing over the n ions in the shell then yields

$$\langle u_i | h_{so} | u_j \rangle = n(\lambda_{ss} + R\lambda_{sp\sigma}/\sqrt{3}) \ . \tag{B12}$$

Evaluation of ϵ_2 is facilitated by using the Hermiticity of h_{so} to transform the first term of Eq. (B2), yielding

$$\epsilon_2 = -N_i N_j[\textstyle\sum_\alpha (S_{\alpha,i}\langle u_j | h_{so} | \varphi_\alpha \rangle)^* + \sum_\beta S_{\beta,j}\langle u_i | h_{so} | \varphi_\beta \rangle] \ . \tag{B13}$$

The matrix elements involving the spin-orbit operator are clearly zero for S-like core states. For P- and D-like states Eq. (B13) is most easily evaluated by considering the products $S_{\alpha,i}\langle u_j | h_{so} | \varphi_\alpha \rangle$ as a unit. For our particularly simple case where both u_i and u_j have spin up, only the L_z component of $\vec{L}$ need be considered.

Substituting for u from Eq. (B5) leads to an expression for $\sum_\alpha S_{\alpha,i}\langle u_j | h_{so} | \varphi_\alpha \rangle$ involving a product of the squares of direction cosines and integrals depending only on the shell radius. For P-like core states, summing over the n ions in a shell yields

$$\textstyle\sum'_\alpha S_{\alpha,i}\langle u_j | h_{so} | \varphi_\alpha \rangle = \tfrac{1}{3}n\sum''_\alpha [S(p_i, p_\alpha\pi)\lambda(p_j, p_\alpha\pi) + S(p_i, p_\alpha\pi)\lambda(p_j, p_\alpha\sigma) + S(p_i, p_\alpha\sigma)\lambda(p_j, p_\alpha\pi)] \ . \tag{B14}$$

Here the λ's are similar to overlap integrals, but include the ionic spin-orbit interaction. They are conveniently defined in terms of an ion of the z axis and are

$$\lambda(p_j, p_\alpha\sigma) = \tfrac{1}{2}\hbar^2 \int \mathcal{R}_j(r)Y_{1,0}(\vec{r})\xi(r)\mathcal{R}_\alpha(r)Y_{1,0}(\vec{r})\,d^3r \tag{B15}$$

and

$$\lambda(p_j, p_\alpha\pi) = \tfrac{1}{2}\hbar^2 \int \mathcal{R}_j(r)Y_{1,1}(\vec{r})\xi(r)\mathcal{R}_\alpha(r)Y_{1,1}(\vec{r})\,d^3r \ . \tag{B16}$$

For the D-like core states the sum over the shell of ions is

$$\textstyle\sum'_\alpha S_{\alpha,i}\langle u_j | h_{so} | \varphi_\alpha \rangle = \tfrac{1}{3}n\sum''_\alpha [S(p_i, d_\alpha\pi)\lambda(p_j, d_\alpha\pi) + \sqrt{3}\,S(p_i, d_\alpha\pi)\lambda(p_j, d_\alpha\sigma) + \sqrt{3}\,S(p_i, d_\alpha\sigma)\lambda(p_j, d_\alpha\pi)] \ , \tag{B17}$$

where the λ's are similar to those defined by Eqs. (B15) and (B16), but with $Y_{1,0}(\vec{r})$ replaced with $Y_{2,0}(\vec{r})$ and $Y_{1,1}(\vec{r})$ replaced with $Y_{2,1}(\vec{r})$.

The ion-ion term ϵ_3 may be handled in exactly the same manner as the vacancy-ion terms in Eq. (B13). The result for P-like core states is

$$\textstyle\sum'_{\alpha,\beta} S_{i,\alpha}S_{\beta,j}\langle \varphi_\alpha | h_{so} | \varphi_\beta \rangle = \tfrac{1}{3}n\sum''_{\alpha,\beta}\lambda_{\alpha,\beta}[S(p_i, p_\alpha\pi)S(p_j, p_\beta\pi) + S(p_i, p_\alpha\pi)S(p_j, p_\beta\sigma) + S(p_i, p_\alpha\sigma)S(p_j, p_\beta\pi)] \ . \tag{B18}$$

A similar result holds for the D-like core states, but as in Eq. (B17) an additional multiplicative factor of $\sqrt{3}$ occurs in the terms involving products of σ and π overlaps. In both expressions $\lambda_{\alpha\beta}$ is the ionic spin-orbit integral given by

$$\lambda_{\alpha\beta} = i\int [\mathcal{R}_\alpha(r)Y_{L(\alpha),\bar{1}}(\vec{r})\downarrow]\,h_{so}[\mathcal{R}_\beta(r)Y_{L(\beta),1}(\vec{r})\uparrow]\,d^3r = \delta_{L(\alpha),L(\beta)}\,\tfrac{1}{2}\hbar^2\int_0^\infty \mathcal{R}_\alpha(r)\mathcal{R}_\beta(r)\xi(r)r^2\,dr \ , \tag{B19}$$

where δ is the Kronecker-δ symbol.

---

*Work supported in part by grants from the National Science Foundation and in part by the U. S. AEC.

†On assignment from the Solid State Science Division, Argonne National Laboratory to Michigan State University for the 1971–1972 academic year.

[1]N. V. Karlov, J. Margerie, and Y. Merle d'Aubigné, J. Phys. (Paris) 24, 717 (1963).

[2]F. Lüty and J. Mort, Phys. Rev. Letters 12, 45 (1964).

[3]R. Romestain and J. Margerie, Compt. Rend. 258, 2525 (1964).

[4]J. Margerie and R. Romestain, Compt. Rend. 258, 4490 (1964).

[5]J. Gareyte and Y. Merle d'Aubigné, Compt. Rend. 258, 6393 (1964).

[6]J. Mort, F. Lüty, and F. C. Brown, Phys. Rev. 137, A566 (1965).

[7]C. H. Henry, Phys. Rev. 140, A256 (1965).

[8]F. C. Brown, B. C. Cavenett, and W. Hayes, Proc. Roy. Soc. (London) A300, 78 (1967).

[9]J. Margerie, J. Phys. (Paris) 28, Suppl. C4-103 (1967).

[10]M. P. Fontana, Phys. Rev. B 2, 1107 (1970).

[11]S. E. Schnatterly, Phys. Rev. 140, A1364 (1965).

[12]C. H. Henry, S. E. Schnatterly, and C. P. Slichter, Phys. Rev. 137, A583 (1965).

[13]C. H. Henry and C. P. Slichter, in *Physics of Color Centers*, edited by W. B. Fowler (Academic, New York, 1968), Chap. 6.

[14]P. R. Moran, Phys. Rev. 137, A1016 (1965).

[15]Y. Merle d'Aubigné and J. Gareyte, Compt. Rend. 261, 689 (1965); Proceedings of the International Symposium on Color Centers in Alkali Halides, Urbana, Ill., 1965, abstract No. 37 (unpublished).

[16]F. C. Brown, B. C. Cavenett, and W. Hayes, Phys. Letters 19, 167 (1965).

[17]E. Krätzig and W. Staude, Phys. Letters 26A, 133 (1968).

[18]E. Krätzig and W. Staude, Phys. Status Solidi 36, 273 (1969).

[19]F. Lüty, Z. Physik 160, 1 (1960).

[20]D. Y. Smith and G. Spinolo, Phys. Rev. 140, A2121 (1965), and references cited therein.

[21]G. Chiarotti and U. M. Grassano, Phys. Rev. Letters 16, 124 (1966); Nuovo Cimento B46, 78 (1966).

[22]N. F. Mott and R. W. Gurney, *Electronic Processes in Ionic Crystals* (Oxford U. P., New York, 1940), p. 114.

[23]R. F. Wood, Phys. Rev. Letters 11, 202 (1963).

[24]G. Spinolo and D. Y. Smith, Phys. Rev. 140, A2117 (1965), and references cited therein.

[25]R. S. Crandall and M. Mikkor, Phys. Rev. 138, A1247 (1965).

[26]F. Nakazawa and H. Kanzaki, J. Phys. Soc. Japan 22, 844 (1967).

[27]K. Maier and W. Gebhardt, Phys. Status Solidi 27, 713 (1968).

[28]See, for example, B. S. Gourary and F. J. Adrian, in *Solid State Physics*, edited by F. Seitz and D. Turnbull (Academic, New York, 1960), Vol. 10.

[29]W. B. Fowler, in *Physics of Color Centers*, edited by W. B. Fowler (Academic, New York, 1968), Chap. 2.

[30]M. Wagner, Z. Naturforsch. 15a, 889 (1960); 16a, 302 (1961).

[31]G. Iadonisi and B. Presiosi, Nuovo Cimento B48, 92 (1967).

[32]H. Seidel and H. C. Wolf, in *Physics of Color Centers*, edited by W. B. Fowler (Academic, New York, 1968), Chap. 8.

[33]See, for example, W. Kohn, in *Solid State Physics*, edited by F. Seitz and D. Turnbull (Academic, New York, 1957), Vol. 5.

[34]D. Y. Smith, Phys. Rev. 137, A574 (1965).

[35]D. Y. Smith, Solid State Commun. 8, 1677 (1970).

[36]L. I. Schiff, *Quantum Mechanics*, 2nd ed. (McGraw-Hill, New York, 1949).

[37]Note the correction of a sign error in Eq. (4) of Ref. 34. Unfortunately, this misprint has propagated to a review article; see Ref. 29, p. 95.

[38]J. C. Slater and G. F. Koster, Phys. Rev. 94, 1498 (1954), especially p. 1503.

[39]Note that these matrix elements reduce to the diagonal-element formulas of Ref. 34 when $i=j$.

[40]E. U. Condon and G. H. Shortley, *Theory of Atomic Spectra* (Cambridge U. P., London, 1957).

[41]Reference 36, p. 290.

[42]See Table IV and the discussion in Sec. IV.

[43]See, for example, J. Callaway, *Energy Band Theory* (Academic, New York, 1964).

[44]R. E. Watson and A. J. Freeman, Phys. Rev. 124, 1117 (1961).

[45]D. R. Hartree and W. Hartree, Proc. Roy. Soc. (London) A156, 45 (1936).

[46]In the present paper the off-diagonal spin-orbit matrix element is given in terms of $\langle \phi_{n\rho}^{3/2,3/2} | h_{so} | \phi_{m\rho}^{3/2,3/2} \rangle$ rather than as the product of a spin-orbit parameter λ_{KF} and the off-diagonal orbital momentum matrix element $\langle y_K | L_z | x_F \rangle$, as in Ref. 18. The present preference for the first form is that the spin-orbit operator is $\xi(\vec{r})\vec{L}\cdot\vec{S}$ and its matrix element cannot be written as $\lambda\vec{L}\cdot\vec{S}$. This practice arises from elementary atomic spectroscopy, in which wave functions are eigenstates of L_z and S_z, so that $\langle \varphi_i | \xi(\vec{r})\vec{L}\cdot\vec{S} | \varphi_j \rangle = \delta_{ij}\langle \varphi_j | \xi(\vec{r}) | \varphi_j \rangle \langle j | L_z | j \rangle \langle j | S_z | j \rangle$. However, in a crystal L_z is not a good quantum number and it seems artificial to divide the spin-orbit matrix element into the product form.

[47]J. H. Schulman and W. D. Compton, *Color Centers in Solids* (MacMillan, New York, 1962).

[48]Iadonisi and Preziosi find good agreement with the observed spectra for $\epsilon = 2.19$; see Ref. 31.

[49]See, for example, M. I. Petrashen', I. V. Abarenkov, and N. N. Kristofel', Opt. i Spectroskopiya 9, 527 (1960) [Sov. Phys. Opt. Spectry. 9, 276 (1960)].

[50]D. Y. Smith (unpublished).

[51]E. Brown, Phys. Rev. 126, 421 (1962).

[52]The shape function is proportional to optical-absorption coefficient divided by the absorption energy. For a discussion see Sec. III of Ref. 12.

[53]Note the difference in sign between these results and the formulas of Ref. 18. This arises because of a confusion in the definition of right- and left-circular polarization in early work on the subject. For the correct definition see Ref. 13, p. 356. Experimental results taken from Ref. 18 for use in this paper have been corrected for this sign error.

[54]D. Y. Smith and D. L. Dexter, in *Progress in Optics*, Vol. X, edited by E. Wolf (North-Holland, Amsterdam, to be published), especially Fig. 5.

[55]Y. Merle d'Aubigné, as quoted by J. Margerie, Ref. 9.

[56]The value quoted in the present work for Δ_F in RbCl as measured by Faraday rotation differs from the published value by a small correction for diamagnetic effects [F. C. Brown (private communication)].

[57]B. S. Gourary and F. J. Adrian, Phys. Rev. 105, 1180 (1957).

[58]P. O. Löwdin, Advan. Phys. 5, 1 (1956).